ChemElectroChem

Review
doi.org/10.1002/celc.202500052

Chemistry Europe
European Chemical Societies Publishing

www.chemelectrochem.org

Electrodeposition of Thermoelectric Materials

Samuel C. Perry,* Samina Akbar, Robert Clarke, Syed Z. H. Shah, and Iris Nandhakumar

Thermoelectric (TE) materials produce electrical energy when exposed to a thermal gradient and so have unsurprisingly gathered increasing interest as a promising tool in the route to reduced carbon energy emissions. However, many synthetic routes currently involve high-temperatures, oxygen-free environments and harsh chemical reagents. Electrochemistry offers an attractive alternate synthetic route for similar materials at greatly reduced temperatures, without the need for strong chemical reductants. This review looks at recent developments in the electrodeposition of TE materials, highlighting promising materials and techniques. It also outlines key challenges that must be addressed in order to advance the readiness of this technology for wider implementation.

1. Introduction

Thermoelectric (TE) materials enable the conversion of thermal and electrical energy through the Seebeck and Peltier effects. As such, TE devices have gained significant attention in recent years due to their potential for sustainable energy harvesting and cooling applications. These solid-state devices offer advantages such as compact size, scalability, zero emissions, and low maintenance requirements since they contain no moving parts. Efforts to enhance the efficiency of TE materials focus on improving their figure of merit, zT

$$zT = \frac{S^2\sigma T}{\kappa} \tag{1}$$

where σ is the electrical conductivity, S is the Seebeck coefficient, κ is the thermal conductivity, and T is the absolute temperature.[1] A higher zT value indicates a better TE performance. This requires maximizing the power factor, PF

$$PF = S^2\sigma$$

while simultaneously minimizing the thermal conductivity. This is the key challenge in the field, since the two parameters are often interdependent. The optimization of one can therefore have a deleterious impact on the other. For example, increasing carrier concentration can enhance electrical conductivity but typically reduces the Seebeck coefficient and increases electronic thermal conductivity.[2] Intensive efforts have therefore been dedicated to devising novel techniques and approaches to decouple electrical conductivity, Seebeck coefficient, and thermal conductivity, aiming to increase zT.

The zT values are highly dependent on the operating temperatures of TE materials. For example, $Bi_{1-x}Sb_x$ alloys exhibit optimal performance near liquid nitrogen temperatures, making them suitable for low-temperature applications.[3] The highest figure of merit for TE materials has been reported for Bi_2Te_3-based compounds, particularly for applications near room temperature, making them suitable for industrial use in that range.[4] PbTe and $CoSb_3$-based alloys show improved performance around 600 K, making them suitable for power generation applications.[5] Considering these ranges, the operating temperatures of commercial TE generation modules (TEGs) show great potential for implementing heat recovery systems in various processes.

A broad range of techniques have been investigated for the production of TE materials, each with its own advantages and drawbacks. Chemical vapor deposition enables the formation of pure and unfiorm films but comes with high equipment and operating costs.[6] Solvothermal synthesis offers good control of alloy stoichiometry and options for nanostructuring, but requires harsh chemical reductants and careful management of an oxygen-free environment.[7] Mechanical alloying is a versatile technique for room temperature materials synthesis but offers limited structural control over important features such as particle size, and does not offer routes to 1D nanostructures that are of growing interest in the field.[8]

Among these methods, electrodeposition stands out as a promising approach. Electrodeposition uses an electrical current to convert a solution-phase precursor into a solid material at an electrode surface. Electrodeposition typically operates at room temperature, minimizing interdiffusion and preventing undesirable chemical reactions.[9] It has low equipment costs and is material-efficient with minimal wastage, making it a cost-effective method for device fabrication.

Electrodeposition enables precise control over the morphology, composition, and crystallinity of materials through the adjustment of electrodeposition parameters. Moreover, the scalability of electrodeposition for both macroscopic and microscopic areas, combined with deposition rates reaching several tens of microns per hour, provides substantial economic advantages for industrial applications.

S. C. Perry, S. Akbar, R. Clarke, S. Z. H. Shah, I. Nandhakumar
Department of Chemistry and Chemical Engineering
University of Southampton
University Road, Southampton SO17 1BJ, UK
E-mail: S.C.Perry@soton.ac.uk

It is also highly versatile. The application can be manipulated via the applied potential, current, deposition time, precursor species, and solvent, giving the user a large scope of controls over the produced material. For BiTe alloys, film composition is strongly dependent upon applied potential. More negative potential leads to Te rich nonstoichiometric deposits. Grain morphology can also change from single to multiorder platelets when more negative deposition potentials are applied, leading to decreased texture intensity. A pronounced shift in surface morphology is observed from granular in stoichiometric or Bi-rich films to needle-like in Te-rich compositions. These structural transformations significantly alter electrical resistivity and carrier concentration. Hall mobility decreases with increasing carrier concentration. For electrodeposited TE films, the Seebeck coefficient has been shown to enhance significantly with increasing electrical conductivity, as shown in **Figure 1**.[10]

Working solutions can be aqueous or nonaqueous, allowing the creation of metals, semiconductors, and polymers in various forms. Produced materials may be thin film, mesoporous, or nanostructured films with precisely controlled thicknesses, ranging from the nanoscale to several millimeters, by monitoring the consumed charge.

Integrating thin-film TE devices into microsystems aims to deliver high cooling power within compact areas. In contrast, thick-film TE devices are better suited for larger surface areas and work well under small to moderate temperature differences. The current density scales with material thickness and must be optimized to ensure efficient and economical device operation.[11]

2. Electrodeposition for TE Materials

2.1. Materials Scope

At its simplest, electrodeposition of a precursor material can be used to create a solid thin film at an electrode surface. Since the deposition rate is related to the standard potential of the precursor species (E^0). So long as the values for E^0 are fairly similar, multiple precursors can be deposited simultaneously in order to build up thin films of complex binary alloys and ternary alloys (**Table 1**). The impact of differences in E^0 on stoichiometry can be compensated for by tuning the relative concentrations of each precursor compound in solution. Combinatorial manipulation of both the

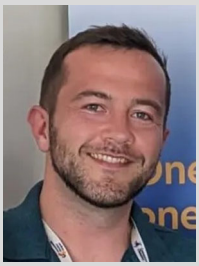

Samuel C. Perry is a teaching fellow at University of Southampton with responsibilities for leading practical physical chemistry education. His research interests span chemical and pedagogical goals in physical chemistry. He has extensive experience in the application of electrochemistry to challenges in sustainable practices, including carbon sequestration, electrodeposition of thermoelectric (TE) materials, and electrosynthesis of hydrogen peroxide. He is also actively involved in curriculum design to provide inclusive chemistry education environments and support students through stress, anxiety, and wellbeing.

Samina Akbar is a highly skilled and results-driven chemist, currently working at the School of Chemistry, University of Southampton, UK. She earned her PhD from the University of Reading, UK, in 2012. During her PhD, Dr. Akbar pioneered a fabrication approach that produced nanostructured platinum with entirely new morphology. This innovation has led to several high-profile publications and contributed significantly to advances in nanomaterials research. Her current work focuses on the fabrication of 3D TE materials. Her research spans a wide range of applications, including fuel cells, batteries, power generation, consumer electronics, and pharmaceuticals.

Robert Clarke is a postgraduate researcher affiliated with the University of Southampton, Diamond Light Source, and ISIS Neutron and Muon Source. He obtained his integrated master's degree from the University of Southampton in 2022. His current research is focused on the novel synthesis of TE metal-organic frameworks.

Syed Z. H. Shah recently completed his Ph.D. in Chemistry through a joint doctoral program between the University of Southampton, UK, and the Institute of Materials Research and Engineering (IMRE), Singapore. He earned his master's degree in nanotechnology from the Royal Institute of Technology (KTH), Sweden, in 2020. From 2020 to 2024, Dr. Syed pursued his doctoral research with a focus on the development of organic-inorganic hybrid composite TE materials. His interdisciplinary expertise bridges materials science, nanotechnology, and applied chemistry, contributing to advancements in sustainable energy technologies.

Iris Nandhakumar is currently an associate professor at the University of Southampton. She received a first-class Dipl.-Chem. degree from the Technical University of Berlin and gained her PhD in Chemistry at the University of Southampton. She also holds an MPhil in Physics from the University of Cambridge, Cavendish Laboratory. Her research focuses on the fabrication and characterization of nanoscale materials, in particular the electrochemical deposition of TE materials and she has more than 75 publications in the area.

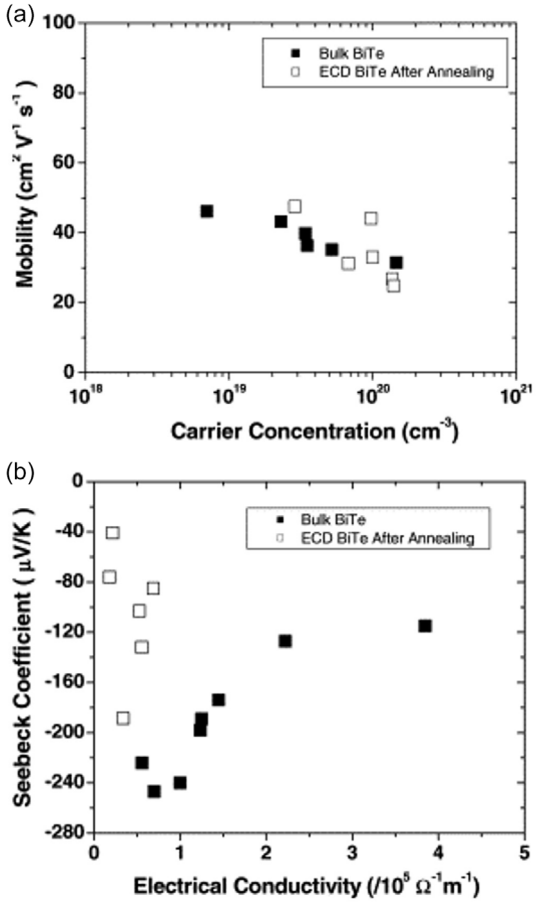

Figure 1. a) Dependence of in-plane hall mobility of Bi_xTe_y electrodeposits on carrier concentrations. b) Dependence of Seebeck coefficient of Bi_xTe_y electrodeposits on electrical conductivity. Adapted with permission.[10] Copyright 2005, Elsevier.

concentrations and applied potential therefore offers a straightforward route to precise stoichiometries of complex materials (**Figure 2**).

This is vital for materials development, as stoichiometry directly impacts TE properties through modulation of charge carrier concentrations, band structure, and thermal conductivity.[12,13] Alternatively, alloyed materials can also be made by electrodepositing one material and then using a second postdeposition step to introduce an alloying element,[14] although this work will focus on purely electrochemical methodologies.

The flexibility of electrodeposition as a technique means that the scope of TE materials produced is extremely broad. Most focus on codeposition of chalcogenides with bismuth, antimony or lead.[15,16] Other options include the deposition of TE metal organic frameworks (MOFs)[17] or organic TE polymers.[18]

2.2. Electrodeposition Conditions

The choice of electrodeposition mode may impact the structure and stoichiometry, providing users with a high degree of control over the resultant material. Constant potential (chronoamperometry) deposition maintains a fixed electrical potential throughout deposition. This offers good control over film composition and stoichiometry and tends to produce more compact films due to the constant driving force for the reduction.[19] Conversely, constant current (chronopotentiometry) deposition applies a fixed current. This gives a more consistent growth rate that allows thickness control through a programmed deposition time but offers less control over stoichiometry and can produce more porous, dendritic, or defect-dense structures.[16]

Pulse electrodeposition (PED) involves switching between two potentials, a short deposition pulse followed by a longer relaxation pulse. Adjusting pulse parameters allows the diffuse layer to recover, enabling precise tuning of deposit stoichiometry and microstructure.[20] This method has been found to improve the mechanical and electrical properties of the various materials, relative to potentio- or galvanostatic methods, including BiTe,[21] SnSe,[22,23] and BiSbTe.[24] PED has also been employed for deposition through porous templates. The rest pulse allows the pores to "refill" with precursor via diffusion, improving pore filling and maintaining stoichiometry throughout the nanostructure.[25]

TE materials may also be deposited via electroless deposition. Here, the driving force is provided by an electrically connected sacrificial anode, which oxidatively dissolves, driving the concurrent deposition of the TE material. This method has more commonly been used for surface modification of existing TE materials,[26] although it has been successfully employed to produce metallic TE materials such as Te nanowires.[27]

2.3. Electrolytes and Deposition Baths

For many TE materials, acid aqueous solutions are preferred choice due to favourable properties, including high precursor solubility, high conductivity, and low viscosity.[28] Electrodeposition of TE materials has been reported from aqueous baths containing nitric acid,[29] perchloric acid,[30] hydrochloric acid,[31] and sulfuric acid.[32] The choice of acid is often made based on the solubility of the constituent cations; for example, nitric acid offers excellent solubility for Bi_2Te_3.

However, aqueous solutions offer some key limitations. These include a narrow potential window, low solubility for certain precursors such as antimony salts,[24] and the poor stability of oxide-based substrates (ITO, SnO_2, SiO_2/Si, etc) in acidic environments.[10] Ionic liquids provide a promising alternative for metal electrodeposition. They offer numerous advantages, including a low melting point, high-thermal stability, high-conductivity, high-solubility for ionic precursors, and negligible vapor pressure.

Eutectic solvents share many of the same advantages. They are typically composed of a quaternary ammonium salt, such as choline chloride, with a hydrogen bond donor, such as a glycol, amide, or carboxylic acid. Eutectic solvents are gaining increased interest over ionic liquids as they come at an often lower toxicity and significantly reduced cost. As such, eutectic solvents have been successfully used for the electrodeposition of a range of TE materials, such as BiTe, CdTe, and SbTe compounds.[33–35]

Table 1. Summary of some recent thin film TE materials produced via electrodeposition. The list is not exhaustive but demonstrates a range of materials that may be made. Table gives quoted values for Seebeck coefficient (S), electrical conductivity (σ), thermal conductivity (κ), power factor (PF) and figure of merit (zT). The temperature where values were recorded (T) is given where a value was reported in the original work. RT indicates room temperature was specified.

Material	S/μV K^{-1}	σ/S m^{-1}	κ/W m^{-1} K^{-1}	PF/μW m^{-1} K^{-1}	zT	T/K	Ref
AgSe	-107 ± 11	301000 ± 1500	0.56 ± 0.06	3421 ± 705	–	298	[102]
$Ag_{3.9}Sb_{33.6}Te_{62.5}$	–	–	1.59	1890	0.95	RT	[103]
$Bi_{0.5}Sb_{1.5}Te_3$	150	10000	–	230	–	RT	[24]
$Bi_{1.6}Te_{3.4}$	−29	403 300	–	340	0.28	RT	[38]
Bi_2Se_3	−62.3	56100	0.76	218	0.09	300	[104]
$Bi_2Te_{2.7}Se_{0.5}$	−92	9500	–	80	–	RT	[105]
Bi_2Te_3	−200	40000	–	1600	–	RT	[106]
CuBiTe	−275	39900	–	3020	–	RT	[107]
BiCuSbTe	152	25000	–	578	–	–	[108]
$Cu_{0.4}SbTe$	−382	20500	–	2800	–	RT	[19]
CuTe	−227	110000	–	5600	–	RT	[109]
$Pb_{49}Te_{51}$	524	14	–	3.9	–	RT	[110]
$Sb_{43.1}Te_{56.9}$	441	28170	–	5480	–	–	[111]
SnSe	–	–	0.34	5.8	–	313	[23]
Te	285	1250	1	280	0.09	RT	[112]
PEDOT[a)]	–	–	0.19	147	0.22	RT	[113]
Polyaniline	30.2	625	–	0.57	–	–	[114]
Polypyrrole	–	–	–	5.23 ± 0.23	0.014 ± 0.0006	–	[115]
Polythiophene	36	70 000	0.21	100	0.1	RT	[116]
$(Cu_3(HHTP)_2$[b)]	−121	0.23	–	0.003	–	301	[17]

[a)]poly(3,4-ethylenedioxythiophene); [b)]Copper 2,3,6,7,10,11-hexahydroxytriphenylene.

3. Controlled Structures in Electrodeposition

3.1. Surfactants

Structural control during electrodeposition can be achieved through a variety of templating methods, depending on the desired level of precision. One of the simplest strategies involves the addition of surfactants or optical brighteners to influence crystal growth. For example, studies on Bi_2Te_3 have shown that various surfactant additives, such as sodium lignosulfate,[36] cetyltrimethylammonium bromide (CTAB),[37] sodium dodecylsulfate (SDS), and polyvinylpyrrolidone (PVP),[38] can give distinct material properties. The choice of surfactant depends on the target outcome; sodium lignosulfate favored growth of the (100) crystallite, CTAB enhanced the mechanical properties of the film, and SDS increased the TE performance.

3.2. Rigid Templates

Nanostructuring is highly desirable in TE materials as a means of enhancing the TE properties. Low-dimensional nanostructures will typically outperform an equivalent thin film.[25] This is down to the combined impact of increased phonon scattering reducing thermal conductivity, while quantum confinement effects can enhance the Seebeck coefficient, thereby increasing zT.[39] Electrodeposition of nanowires is possible through the use of solid-phase templates, most commonly alumina or polycarbonate membranes (**Table 2**). Deposition through these pores produces nanowires, which can then be liberated by dissolving the template.

The same technique can also produce interconnected nanostructures that offer enhanced TE properties thanks to high electrical conductivity and increased thermal scattering.[40] Alternatively, photolithography can etch a pathway through an insulating layer on top of a conductive electrode. Electrodeposition will therefore only occur on the exposed area to give nanowires, or whichever geometry is desired.[41]

The ideal deposition will produce a constant deposit of material, starting at the bottom of the pores, and then evenly growing up the pores and through the template to produce wires. In practical, there are a number of key challenges that interfere with this process. Depositions through porous templates must carefully consider applied overpotential. Potentiostatic depositions involve a nucleation step followed by a growth step. Electrochemical overpotential is the main driving force for nucleation to occur at the bottom of pores. If the overpotential is large and deposition rate is fast, deposition through the wires can become uneven, thus significantly reducing degree of pore filling.[42]

Numerous studies have shown that nucleation does not initiate in every pore, possibly due to variations in surface conditions at the bottom of each pore. The presence of nucleation sites is essential to initiate deposition. This variation leads to uneven pore filling, where some pores complete deposition earlier than others, and many deposits fail to reach the template surface,

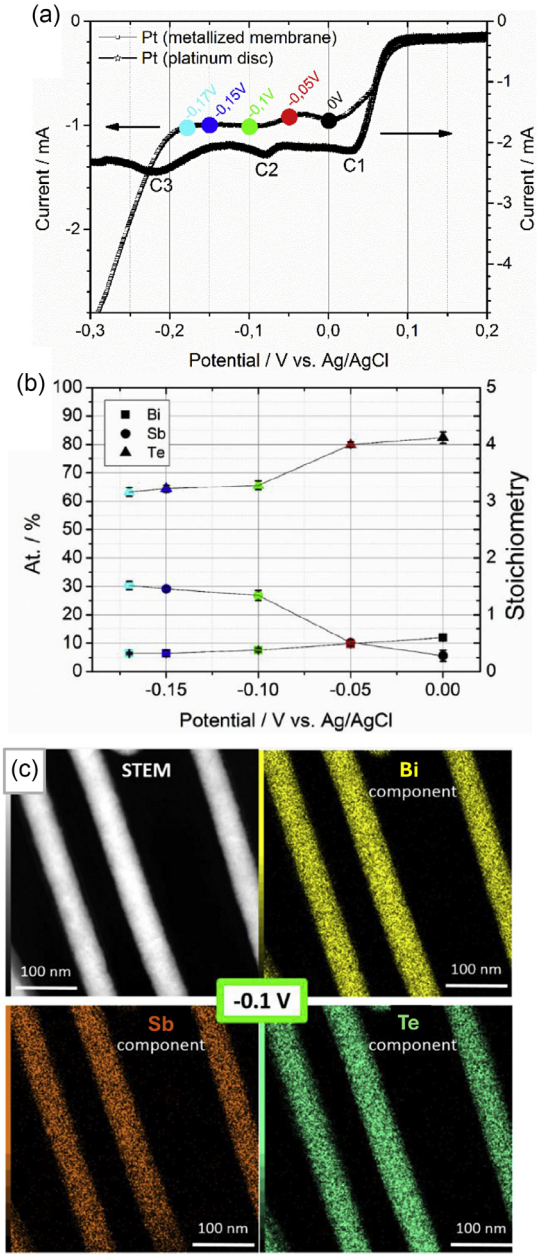

Figure 2. a) 5 mV/s linear sweep voltammogram for 1 M HNO_3, 0.6 M $C_4H_6O_6$, 10 mM $HTeO_2^+$, 1.43 mM Bi^{3+}, 8.58 mM $Sb_2(C_4H_4O_6)_2^{2+}$ at two different geometry platinum electrodes. Peaks C1, C2 and C3 correspond to reduction of Te^{IV} to Te^0, incorporation of Sb and deposition of ternary BiSbTe respectively. Colored circles highlight chosen deposition potentials for the films analyzed in b and c. b) Potential dependence of the composition of $Bi_xSb_yTe_z$ nanowires grown by corresponding fixed potentials, demonstrating how deposition potential impacts the stoichiometry; a more negative deposition potential increases the proportion of Sb at the expense of Bi and Te deposition. c) EDX-TEM measurement for $Bi_{0.4}Sb_{1.3}Te_{3.3}$ deposited at −0.1 V versus SCE. Adapted with permission.[100] Copyright 2018, Elsevier.

resulting in a lower degree of pore filling (defined as the ratio between the average nanowire length and total pore length). Pores that fill quickly will overflow, leading to an exposed island of material at the surface of the template.[43] Further deposition will preferentially occur at this site, leading to the formation of large particles on the template surface and the cessation of further pore filling (**Figure 3**).[44] Deposition rates must therefore be kept low to maintain an even fill rate. Ensuring uniform and simultaneous filling of all template pores remains one of the key challenges in templated nanowire electrodeposition.

For single-element materials, a slow deposition rate may only be an inconvenience in production. However, for binary and ternary materials, this can be significantly challenging, as moving to a lower overpotential to slow the deposition rate will impact the deposition stoichiometry, which can make achieving a specific desired stoichiometry challenging.[45] Reductions in the deposition rate to accommodate pore-fulling must therefore come with a revaluation of deposition bath concentrations.

This situation is further complicated by the isolation deposition solution within the pore. For example, in a solution containing bismuth and tellurium, the deposition may favor bismuth deposition. Initial deposition within the pore would be bismuth-rich and result in a bismuth-depleted solution within pore. Further deposition would then be tellurium-rich, leading to an uneven stoichiometry along the wire.

The same phenomenon can also deleteriously impact single-element materials due to the presence of unwanted side reactions. Depletion of the metal cation precursor within the pore structure would decrease the possible reduction rate, but the same deposition current or potential would still be applied. This causes an acceleration of unwanted background processes such as solvent electrolysis.

All of these issues are exacerbated as pore diameters decrease. Restricted diffusion down narrow pores gives a depleted concentration at the point of deposition, giving nonuniform growth and limiting pore filling.[46] Smaller pores also lead to a higher localized current density at pore openings. This leads to preferential growth at the pore opening rather than within the pore, and leading to pores blocking before filling.[47]

Pulse deposition is a popular solution. The “off” period allows solution within the pores to recover. The entirety of the pore length can then be produced from the same starting concentrations and therefore encourages a uniform stoichiometry. Utilizing this method at 1–4 °C resulted in nanowires achieving 93% pore filling efficiency. Other mediations focus on choice of electrolyte with low viscosity to facilitate pore filling, with some of the thinnest electrodeposited wires produced via electrodeposition from supercritical fluids.[48,49]

3.3. Liquid Crystal Templates

Liquid crystals are materials that exhibit properties between that of a solid and a liquid, meaning that they can flow like a liquid while maintaining an ordered structure. This allows them to act as templates for nanostructured depositions. Coating an electrode with a liquid crystal will cause depositions to occur around the template, which can then be washed away to reveal the templated structure. Liquid crystal templating allows the production of incredibly fine and interconnected nanostructures. The precise structure may be lamellar, cage-type, or hexagonal depending on the concentration and/or composition of the surfactant being

Table 2. Summary of some recent nanostructured TE materials produced via electrodeposition. The list is not exhaustive but demonstrates a range of materials and corresponding morphologies that may be made. Templates are given as either anodized alumina oxide or polycarbonate (PC) membranes. Table gives quoted values for Seebeck coefficient (S), electrical conductivity (σ), thermal conductivity (κ), power factor (PF) and figure of merit (zT). The temperature where values were recorded (T) is given where a value was reported in the original work. RT indicates room temperature was specified.

Material	S/μV K^{-1}	σ/S m^{-1}	κ/W m^{-1} K^{-1}	PF/μW m^{-1} K^{-1}	zT	T/K	Ref
AgSe nanotube	63.9 ± 1.2	373 ± 13.4	–	151.1 ± 13.5	0.40 ± 0.03	RT	[117]
AgTe nanorod	−120	–	–	2451	–	–	[14]
$Bi_{0.5}Sb_{1.5}Te_3$ nanowires	143	480	0.28	700	1.14	330	[118]
$Bi_{0.9}Sb_{0.1}$ nanowires	−80	–	–	–	–	RT	[61]
Bi_2Se_3 micropillars	−162	8.6	–	–	–	RT	[41]
Bi_2Te_3 nanonetwork	−127	30000	0.5	–	–	RT	[40]
Bi_2Te_3 nanowires	55	1690	–	476.3	–	–	[101]
$Bi_{39.4}Te_{61}$ nanowires	−70	4000	–	195.8	–	300	[119]
$Bi_{2.5}Te_{2.78}Se_{0.02}$ nanowires	−60	2700	–	1000	–	300	[120]
PbTe nanowires	–	18100	–	–	–	–	[121]
Sb_2Te_3 nanowires	359	–	–	–	0.09	RT	[122]

used.[50] Relatively few studies have employed liquid crystals for templating TE materials, although examples have been demonstrated for materials including Bi_2Te_3[51] and PbTe.[52]

3.4. Template-Free Nanowires

Template-free electrodeposition of TE nanostructures requires a slow growth rate and coordinating agents in solution to guide growth along a specific crystallographic axis. Ionic liquids and eutectic solvents are particularly effective in this regard, where the choice of component offers good control over the resultant nanostructure.

For example, for a gold electrode in eutectic solvent, the surface-solution interface features an adsorbed cation layer, followed by alternating anion and cation layers.[53] This passivating layer hinders film growth, so once initial nucleation has occurred, further deposition would be strongly preferred at the nucleation site over the passivated surface.[54] Combining this with a naturally anisotropic material such as tellurium facilitates nanowire growth.[55]

Similar effects can be achieved through secondary additives to ionic liquids that strongly bind to either the substrate or to the side of nanowires to encourage axial growth. This has been demonstrated for Sn nanowires, which were electrochemically grown in ionic liquids with $SiCl_4$ as a solution-phase template (**Figure 4).**[56]

Given that the production of wires relies on the anisotropy of the core component, binary and ternary alloys electrodeposited from ionic liquids tend not to produce the same ordered wire structures. Instead, they produce more complex nanostructures, as has been demonstrated for materials such as PbTe,[57] CuTe,[58] and BiSbTe.[59] One workaround to this is through postprocessing. An initial electrodeposition of Te wires could be followed by a second step to introduce a binary element, as has been demonstrated with a secondary electrodeposition of Bi onto Te nanowires, to give a core-shell binary alloy.[60]

3.5. Posttreatment

Postdeposition treatments can dramatically enhance the performance of electrodeposited TE materials. A common method for chalcogenide TE materials is thermal annealing. For nanowire materials, thermal annealing can enhance crystallinity,[61] and improve the contact between neighboring wires, enhancing electrical conductivity.[62] In bulk materials, annealing can reduce defect density and produce a more even distribution of elements within ternary alloys, which in turn increases the Seebeck coefficient.[63] As a result, materials with modest as-deposited properties can yield significantly higher power factors through appropriate posttreatment (**Figure 5).**

4. Additional Materials

4.1. Electrodeposition of Metal-Organic Frameworks

In recent years, novel TE materials have been reported which address the inherent barriers associated with traditional TE such as scarcity, toxicity and rigidity. MOFs are a class of porous materials which have been explored for use in TEGs, whose reticular structures can be tailored to exhibit specific properties. Moreover, due to their porous architecture, they possess intrinsically low thermal conductivity which contributes to a reduced zT value. Electrochemical techniques allow precise control over orientation,[64] film thickness,[65] and crystallinity,[66] which can significantly influence material properties. Postsynthetic approaches have exploited the porous nature of MOFs by introducing redox-active guest molecules to regulate properties like electrical conductivity.[67]

Direct electrodeposition of thin MOF films with enhanced structuring techniques allows for precise control of the crystallite size from 2–50 μm.[65] Depositing as a thin film may provide properties beyond the intrinsic scope of bulk materials, such as decreasing the thermal conductivity parameter.[68] More recently,

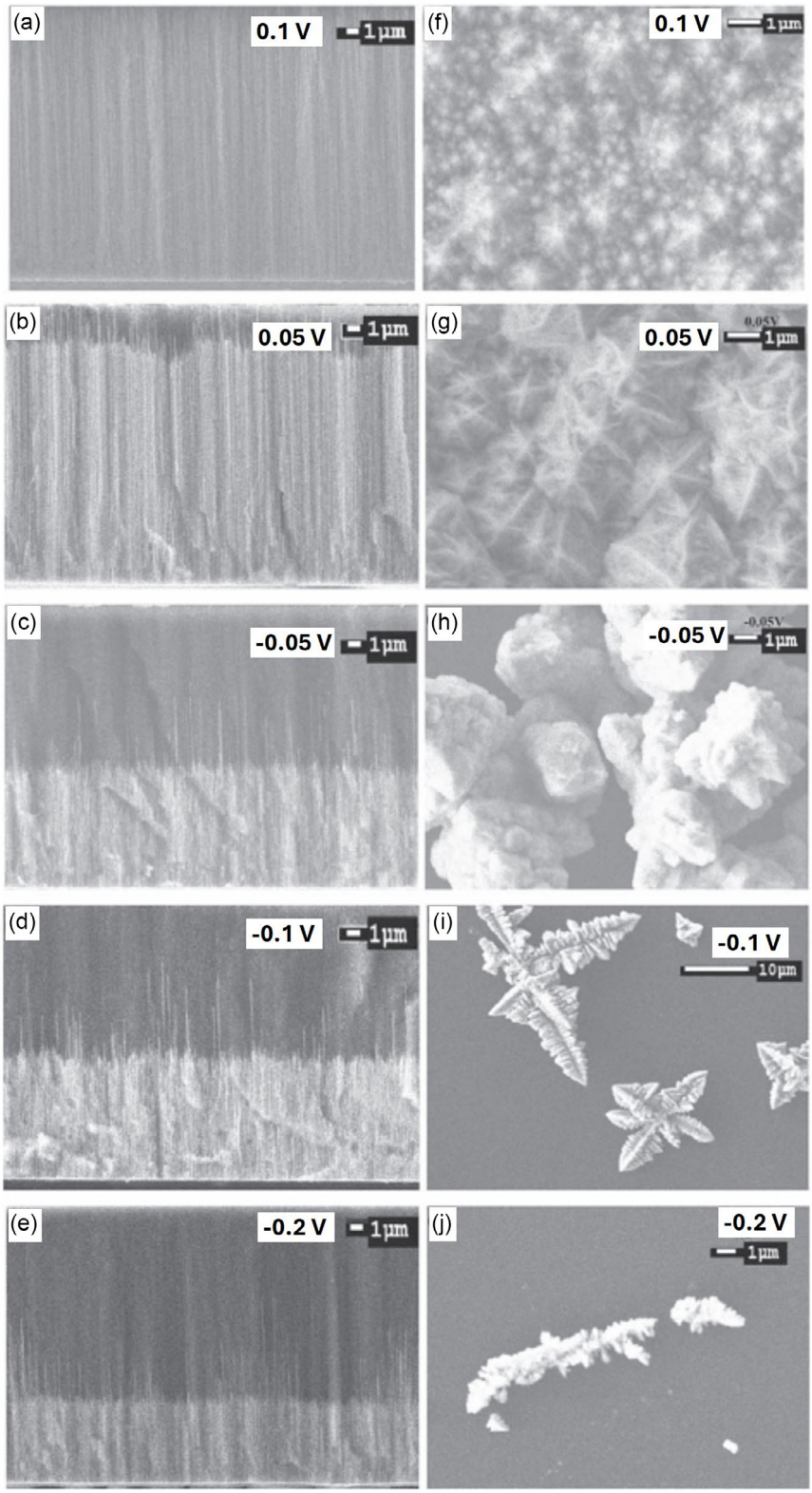

Figure 3. SEM images of nanowires of Bi_2Te_3 deposited within a rigid porous anodized alumina oxide template. Depositions were done at the potential indicated inset of the image. Moving to a more negative potential (larger overpotential) gave a faster deposition rate, which resulted in poorer pore filling and deposition of larger particles at the template surface. Images show the nanowires within the template cross section a–e) and particles formed on the surface of the alumina oxide template. f–j) when deposition was done at the potential indicated inset, with respect to the Ag/AgCl reference electrode. Reproduced with permission.[44] Copyright 2019, IOP Publishing.

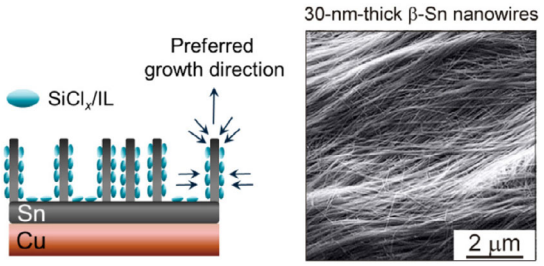

Figure 4. Left, schematic model for the electrodeposition of Sn nanowires from 1-butyl-1-methylpyrrolidinium bis(trifluoromethylsulfonyl)imide(BMP-TFSI) ionic liquid with $SiCl_4$ additive, showing the directing of nanowire growth by $SiCl_4$ adsorption. Right, SEM image of 30 nm diameter Sn nanowires produced via this method. Reproduced with permission.[56] Copyright 2015, American Chemical Society.

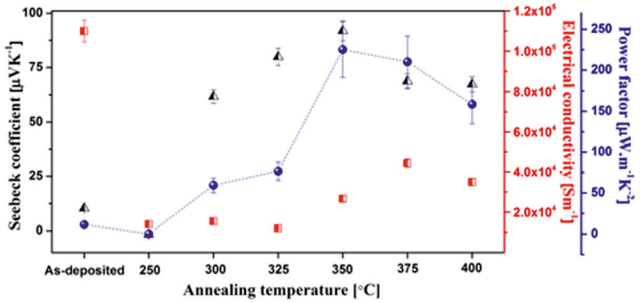

Figure 5. Seebeck coefficient, electrical conductivity, and power factor recorded for electrodeposited BiSbTe films after annealing for 1 h at the given temperature. Annealing gives an initial increase in Seebeck with a decrease in electrical conductivity. Increasing the annealing temperature results in a further increase in Seebeck and an improved electrical conductivity, both of which combine to give a significant improvement in power factor. Adapted under the terms of the Creative Commons License (CC-BY).[101] Copyright 2019, The Authors. Published by AIP Publishing.

research has been focused on the synthesis of 2D-layered *M*-CAT MOFs, based on metal nodes coordinated to aromatic catecholates and analogs. These two constituents coordinate in an extended 2D honeycomb-shaped arrangement, analogous to graphene, and have demonstrated impressive conducting behavior.[69] Control of the anodization potential allows precise regulation of the morphology of nanomaterials, including high aspect-ratio nanorods[64] and nanowires.[66] This manipulation influences electrical and thermal properties through energy filtering mechanisms and the likelihood of phonon scattering.[70]

4.2. Organic TE Polymers

Organic TE polymers offer unique advantges, including low toxicity and inherent flexibility, making them suitable for wearable or biocompatible devices.[71] While electrodeposition is well established for the fabrication of conductive polymers[72] its application of to TE polymers remains comparatively underexplored. Encouragingly, many TE polymers are made up of monomers suitable for electropolymerization, such as polymers of 3-hexylthiophene (P3HT), anailine (PANI), pyrrole (PPy) and 3,4-ethylenedioxythiophene (PEDOT).[73]

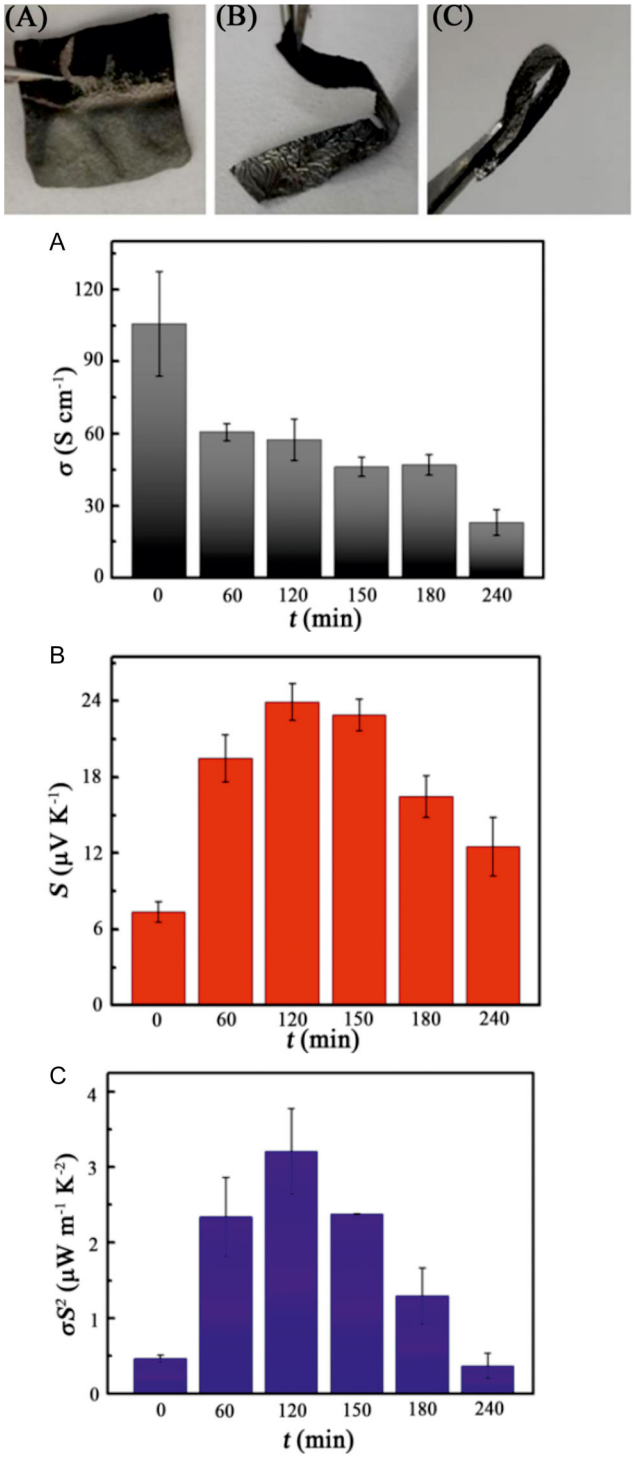

Figure 6. Top row, digital images of polypyrrole/Te films produced by electrodeposition, demonstrating the film flexibility. Columns figures A, B and C show the electrical conductivity (σ), Seebeck coefficient (S) and power factor (σS^2) as a function of Te deposition time onto the polypyrrole film. The film shows the interdependent nature of the parameters; increased Te content decreases conductivity but increases Seebeck up to 120 min, resulting in an optimized power factor at this time. Adapted under the terms of the Creative Commons license, CC-BY-NC-ND.[87] Copyright 2022, The Authors. Published by Elsevier B.V.

Organic TE polymer performance is highly dependent on the incorporation of dopants. These may be ionic dopants that facilitate charge transfer within the polymer, such as

Table 3. Summary of some recent hybrid TE materials produced via electrodeposition. The list is not exhaustive but demonstrates a range of materials and corresponding morphologies that may be made. Table gives quoted values for Seebeck coefficient (S), electrical conductivity (σ), thermal conductivity (κ), power factor (PF) and figure of merit (zT). The temperature where values were recorded (T) is given where a value was reported in the original work. RT indicates room temperature was specified.

Material	S/μV K^{-1}	σ/S m^{-1}	κ/W m^{-1} K^{-1}	PF/μW m^{-1} K^{-2}	zT	T/K	Ref
AgSe/PPy[a)]	–	–	–	282.8 ± 16.5	–	RT	[117]
CNT[b)]/PPy[a)]/Te	–	–	–	1602 ± 87.6	–	300	[123]
CNT[b)]/PPy[a)]/Te/PbTe	41.2 ± 0.1	–	–	929.8 ± 35.4	–	RT	[82]
PANI[c)]/CNTs[b)]	52.5	85000	–	236 ± 5.9	–	RT	[124]
PEDOT[d)]/CNTs[b)]	52.3	400	0.037	1.1	0.009	308	[71]
PEDOT[d)]/SnS/Ag	69	12000	–	58.6	0.05	RT	[86]
PEDOT[d)]/Te/CNTs[b)]	43.4 ± 06	900 ± 20.5	–	169.8 ± 7.8	–	RT	[125]
PPy[a)]/CNTs[b)]	–	–	–	365.2 ± 9.6	0.2 ± 0.005	RT	[126]
PPy[a)]/Te	29	–	–	4.02	–	–	[87]
Sb_2Te_3/CNTs[b)]	45	33000	–	59.5	–	298	[88]
Te/PEDOT[d)]	65.4	561400	–	240	–	300	[84]
TiO_2/PANI[c)]	124	–	–	–	–	303	[89]

[a)]poly(pyrrole), [b)]carbon nanotubes, [c)]poly(aniline), [d)]poly(3,4-ethylenedioxythiophene)

2,3,5,6-tetrafluoro-7,7,8,8-tetracyanoquinodimethane (F4TCNQ),[74] triaminomethanes[75] or $FeCl_3$.[76] This can be achieved through electrochemical doping by biasing the electrode at a positive potential to lead to the accumulation of negative dopant ions.[77] Using the dopant ion as counter ion in the electrolyte during deposition can provide one-step electrochemical doping alongside electrochemical synthesis.[18]

To date, electrochemically synthesized TE polymers tend to underperform versus polymers produced by alternative means. A key challenge is that electrical conductivity is greatly enhanced by the alignment of polymer chains, ordered polymer structures give a significantly enhanced performance.[78] However, alignment is possible through simple postprocessing, with techniques such as high-temperature rubbing showing significant enhancements in power factor.[79] Application of these methods to electrochemically produced TE polymer films could allow these to compete with leading materials.

4.3. Flexible Hybrid Materials

Growing interest in wearable electronics has provided interest in TE materials on flexible substrates. Electrodeposition within flexible nanoporous templates enabled the in situ fabrication of nanowires of Te,[80] Bi_2Te_3,[25] and $Bi_{2-x}Sb_xTe_3$.[81] Flexible films can also be achieved through postprocessing of electrodeposited nanowires. This has been achieved by hot-pressing TE nanowires with carbon[82] and boron nitride nanotubes,[83] and by electrodepositing TE materials directly onto flexible conductive polymers.[84] Selection of the appropriate combination of inorganic core and flexible organic component can elevate the resultant material to give a hybrid TE material (**Figure 6).**

Hybrid TE materials are able to combine the high performance of chalcogenide TE materials along with the flexibility of organic TE materials. These hybrids can exhibit synergistic effects to become greater than the sum of their parts; combining the low thermal conductivity of the organic with the superior charge transfer properties of the inorganic component to give greatly enhanced TE properties.[85] Electrochemical syntheses are well suited to create these hybrids by electrodepositing an inorganic material onto a flexible organic scaffold (**Table 3**). The reverse is also possible, though the benefits of flexible scaffolds for wearable technology applications make this the preferred orientation.

The simplest examples would use a conductive polymer film electrode and deposit nanoparticles of an inorganic TE material within the polymer matrix. This has been demonstrated for AgSn into PEDOT,[86] and Te in polypyrrole.[87] Deposition onto low-dimensional nanostructures such as carbon nanotubes has also been demonstrated.[88] Alternatively, electrochemical deposition can produce an array of nanorods or wires at an electrode surface. If these remain attached, then a second electropolymerization step could connect the nanowires with an interspersed polymer layer to produce a hybrid material, as was demonstrated for polyaniline deposition around electrochemically produced TiO_2 nanotubes.[89]

5. Summary and Outlook

The central challenge for TE materials is to address the optimization of the figure of merit, zT; how to enhance this overall TE performance by increasing the electrical conductivity and Seebeck together, while keeping thermal conductivity low. Achieving this delicate balance is complicated by the inherent interdependence of these parameters. State-of-the-art strategies, including band structure engineering, defect and phonon engineering, nanostructuring, and compositional tuning, have led to significant advances, with some materials now achieving zT values above 2 at elevated temperatures.[90]

The focus of state-of-the-art TE materials will need to balance high-density power generation with viable material choices. Many of the leading materials presently rely on tellurium, which presents challenges with scarcity and toxicity. Selenides have emerged as possible candidates in place of tellurides due to their high-power factor and lower thermal conductivity, coupled with their cost-effectiveness and greater abundance on Earth compared to tellurides.

Alternatively, moving toward organic-based TE materials presents the opportunity to remove costly or toxic chalcogenide precursors, or at least lower the proportion of these needed in a final device. Incorporation of inorganic TE materials into an organic matrix appears to be a promising route to high *zT* values; marrying the benefits of high electronic conductivity of the inorganic with low thermal conductivity in the polymer, as well as lowering costs and adding flexibility.[91]

Combining the high electrical conductivity of inorganics with the low thermal conductivity and mechanical flexibility of polymers enables new device concepts such as wearable and conformable power sources.[92] Recent advances in multicomponent composites and molecular doping strategies have pushed the performance of organic and hybrid TEs closer to that of conventional materials, especially for applications at low and moderate temperatures.[93]

5.1. Industrial Scalability and Manufacturing

For TE materials to move from laboratory innovation to widespread industrial application, scalable and economically viable manufacturing processes are essential. Electrodeposition stands out as a promising technique due to its low equipment cost, material efficiency, and ability to precisely control composition and microstructure. However, several challenges must be addressed for industrial-scale implementation. Current electrodeposition techniques are often limited to batch processing, which restricts throughput. Developing continuous-flow electrodeposition systems, potentially integrated with roll-to-roll manufacturing, could significantly increase production rates and enable the fabrication of large-area TE films and coatings suitable for commercial devices.

Another critical factor for industrial scalability is maintaining bath stability during prolonged operation. This includes managing precursor depletion, byproduct accumulation, and contamination to ensure consistent material quality. The development of advanced monitoring and feedback control systems, along with robust electrolyte formulations, will be crucial to achieving reliable, long-term electrodeposition processes. Furthermore, integrating electrodeposition with additive manufacturing techniques, such as 3D printing, opens exciting possibilities for fabricating complex device architectures and multimaterial systems. Such hybrid manufacturing approaches could enable the direct fabrication of TE modules with embedded cooling features, flexible substrates, or tailored geometries, accelerating the prototyping and deployment of next-generation TE devices.

Beyond traditional inorganic materials, organic and hybrid organic–inorganic TE systems are gaining increasing attention. These materials offer advantages such as mechanical flexibility, low toxicity, and the potential for low-cost, scalable production. Incorporating inorganic TE materials into organic matrices combines the high electrical conductivity of inorganic components with the low thermal conductivity and mechanical compliance of polymers. This synergy enables new device concepts, including wearable and conformable power sources. Recent advances in multicomponent composites and molecular doping have pushed the performance of organic and hybrid TE materials closer to that of conventional inorganic systems, particularly for applications at low to moderate temperatures.

5.2. Emerging Applications

Emerging applications are expanding the scope and impact of TE materials. Flexible and wearable electronics represent a rapidly growing area, where TE materials integrated into textiles, flexible films, and skin-conformable devices can harvest body heat or ambient thermal gradients to power sensors and low-power electronics. Many groups are demonstrating promising prototype devices for power generation using these concepts.[94]

As power factors continue to increase, continued research will look toward miniaturization of these components in order to realize power production for practical devices for Internet of Things and wearable device applications. Demonstrations of flexible TE generators for health monitoring and Internet of Things (IoT) applications highlight the potential of these materials to enable self-powered, autonomous devices.

Additionally, scalable TE modules offer promising opportunities for waste heat recovery in industrial processes, automotive exhaust systems, and consumer electronics, contributing to improved energy efficiency and reduced carbon emissions. Hybrid energy harvesting systems that integrate TE with photovoltaics, piezoelectrics, or other technologies may provide more versatile and robust solutions by capturing multiple ambient energy sources simultaneously.

5.3. Future Research Directions

To accelerate the transition of TE materials from laboratory to real-world applications, several research priorities should be emphasized. Continued exploration of earth-abundant, nontoxic materials, such as selenides, sulfides, and organic semiconductors, is critical for sustainable and scalable TE solutions.[95] Advances in microstructural engineering, including precise control of nanostructures, defect densities, and interfaces, will further decouple electrical and thermal transport properties, enabling higher *zT* values.[96]

The application of machine learning and high-throughput computational screening promises to accelerate the discovery and optimization of new TE materials by predicting promising compositions and processing conditions.[97,98] Moreover, research must extend beyond materials development to focus on device integration, module architecture, and system-level optimization to maximize real-world efficiency and reliability.

Sustainable manufacturing practices will also play a vital role in the long-term success of TE technologies. Developing green, energy-efficient, and low-waste production methods, along with strategies for recycling and reprocessing TE materials, will be necessary to minimize environmental impact and support circular economy principles.[99]

In summary, the future of TE materials is increasingly interdisciplinary, combining innovations in chemistry, materials science, engineering, and data science. As material performance continues to improve and scalable manufacturing techniques mature, TE materials are poised to play a transformative role in energy harvesting, waste heat recovery, and next-generation electronics. The integration of electrodeposition with advanced manufacturing technologies and the rise of flexible, hybrid, and organic TE materials will further expand the application landscape, paving the way for ubiquitous, sustainable, and adaptable energy solutions.

Acknowledgements

The authors would like to acknowledge financial support from the Engineering and Physical Sciences Research Council, Grants EP/T026219/1 and EP/X012840/1.

Conflict of Interest

The authors declare no conflict of interest.

Keywords: electrodepositions · energy · hybrid materials · nanostructures · TE

[1] G. D. Mahan, *APL Mater.* **2016**, *4*, 104806.
[2] W. G. Zeier, A. Zevalkink, Z. M. Gibbs, G. Hautier, M. G. Kanatzidis, G. J. Snyder, *Angew. Chem. Int. Ed.* **2016**, *55*, 6826.
[3] S. Gao, J. Gaskins, X. Hu, K. Tomko, P. Hopkins, S. J. Poon, *Sci. Rep.* **2019**, *9*, 14892.
[4] Y. Sun, F. Guo, Y. Feng, C. Li, Y. Zou, J. Cheng, X. Dong, H. Wu, Q. Zhang, W. Liu, Z. Liu, W. Cai, Z. Ren, J. Sui, *Nat. Commun.* **2023**, *14*, 8085.
[5] S. Wan, Q. Song, H. Chen, Q. Zhang, J. Liao, X. Xia, C. Wang, P. Qiu, B. Chen, S. Bai, L. Chen, *Cell Rep. Phys. Sci.* **2023**, *4*, 101651.
[6] D. W. Newbrook, S. P. Richards, V. K. Greenacre, A. L. Hector, W. Levason, G. Reid, C. H. de Groot, R. Huang, *J. Alloy Comp.* **2020**, *848*, 156523.
[7] A. Amin, R. Huang, D. Newbrook, V. Sethi, S. Yong, S. Beeby, I. Nandhakumar, *J. Phys. Energy* **2022**, *4*, 024003.
[8] B. K, S. P. D, S. M, S. J B, F. K, R. P, *Solid State Sci.* **2024**, *157*, 107721.
[9] M. B. Kale, R. A. Borse, A. Gomaa Abdelkader Mohamed, Y. Wang, *Adv. Func. Mater.* **2021**, *31*, 2101313.
[10] B. Yoo, C.-K. Huang, J. Lim, J. Herman, M. Ryan, J.-P. Fleurial, N. Myung, *Electrochim. Acta* **2005**, *50*, 4371.
[11] S. Li, M. S. Toprak, H. M. A. Soliman, J. Zhou, M. Muhammed, D. Platzek, E. Müller, *Chem. Mater.* **2006**, *18*, 3627.
[12] Y. Zheng, T. J. Slade, L. Hu, X. Y. Tan, Y. Luo, Z.-Z. Luo, J. Xu, Q. Yan, M. G. Kanatzidis, *Chem. Soc. Rev.* **2021**, *50*, 9022.
[13] Y. Jiang, J. Dong, H.-L. Zhuang, J. Yu, B. Su, H. Li, J. Pei, F.-H. Sun, M. Zhou, H. Hu, J.-W. Li, Z. Han, B.-P. Zhang, T. Mori, J.-F. Li, *Nat. Commun.* **2022**, *13*, 6087.
[14] K. Al Hokayem, J. Ghanbaja, S. Michel, S. Legeai, N. Stein, *Mater. Chem. Phys.* **2022**, *289*, 126487.
[15] J. Wei, L. Yang, Z. Ma, P. Song, M. Zhang, J. Ma, F. Yang, X. Wang, *J. Mater. Sci.* **2020**, *55*, 12642.
[16] T. Wu, J. Kim, J.-H. Lim, M.-S. Kim, N. V. Myung, *Front. Chem.* **2021**, *9*.
[17] M. de Lourdes Gonzalez-Juarez, E. Flores, M. Martin-Gonzalez, I. Nandhakumar, D. Bradshaw, *J. Mater. Chem. A* **2020**, *8*, 13197.
[18] S. C. Perry, S. Arumugam, S. Beeby, I. Nandhakumar, *J. Electronal. Chem.* **2023**, *933*, 117278.
[19] A. Tanwar, R. Kaur, N. Padmanathan, K. M. Razeeb, *Sustain Energy Fuel* **2023**, *7*, 4160.
[20] M. Okuhata, D. Takemori, M. Takashiri, *ECS Trans.* **2017**, *75*, 133.
[21] C. Lei, K. S. Ryder, E. Koukharenko, M. Burton, I. S. Nandhakumar, *Electrochem. Commun.* **2016**, *66*, 1.
[22] M. De Vos, A. Zimmer, M. Toledo, J. Ghanbaja, E. Haye, G. Pernot, D. Lacroix, N. Stein, *Appl. Surf. Sci.* **2023**, *621*, 156845.
[23] M. R. Burton, C. A. Boyle, T. Liu, J. McGettrick, I. Nandhakumar, O. Fenwick, M. J. Carnie, *ACS Appl. Mater. Interface* **2020**, *12*, 28232.
[24] C. Lei, M. Burton, I. S. Nandhakumar, *J. Electrochem. Soc.* **2017**, *164*, D192.
[25] P. Cervino-Solana, M. J. Ramirez-Peral, M. S. Martín-González, O. Caballero-Calero, *Heliyon* **2024**, *10*, e36114.
[26] K. Kohashi, Y. Okano, D. Tanisawa, K. Kaneko, S. Miyake, M. Takashiri, *Crystals* **2024** *14*, 132.
[27] S. C. Perry, J. White, I. Nandhakumar, *RSC Adv.* **2022**, *12*, 35938.
[28] V. S. Khairnar, A. N. Kulkarni, V. V. Lonikar, N. D. Jadhav, D. P. Patil, A. B. Gite, M. Kumar, *J. Mater. Sci.: Mater. Electron.* **2024**, *35*, 1344.
[29] J. Recatala-Gomez, P. Kumar, A. Suwardi, A. Abutaha, I. Nandhakumar, K. Hippalgaonkar, *Sci. Rep.* **2020**, *10*, 17922.
[30] D. Del Frari, S. Diliberto, N. Stein, C. Boulanger, J.-M. Lecuire, *Thin Solid Films* **2005**, *483*, 44.
[31] F. Li, W. Wang, *Appl. Surf. Sci.* **2009**, *255*, 4225.
[32] P. Heo, K. Hagiwara, R. Ichino, M. Okido, *J. Electrochem. Soc.* **2006**, *153*, C213.
[33] F. Golgovici, T. Visan, *Chalcogenide Lett.* **2012**, *10*, 427.
[34] F. Golgovici, A. Cojocaru, M. Nedelcu, T. Visan, *Chalcogenide Lett.* **2009**, *6*, 323.
[35] F. Golgovici, T. Visan, *Chalcogenide Lett.* **2012**, *9*, 165.
[36] A. J. Naylor, E. Koukharenko, I. S. Nandhakumar, N. M. White, *Langmuir* **2012**, *28*, 8296.
[37] Y. Song, I.-J. Yoo, N.-R. Heo, D. C. Lim, D. Lee, J. Y. Lee, K. H. Lee, K.-H. Kim, J.-H. Lim, *Curr. Appl. Phys.* **2015**, *15*, 261.
[38] C. Kulsi, M. Mitra, K. Kargupta, S. Ganguly, D. Banerjee, S. Goswami, *Mater. Res. Exp.* **2015**, *2*, 106403.
[39] M. Muñoz Rojo, B. Abad, C. V. Manzano, P. Torres, X. Cartoixà, F. X. Alvarez, M. Martín Gonzalez, *Nanoscale* **2017**, *9*, 6741.
[40] A. Ruiz-Clavijo, O. Caballero-Calero, C. V. Manzano, X. Maeder, A. Beardo, X. Cartoixà, F. X. Álvarez, M. Martín-González, *ACS Appl. Energy Mater.* **2021**, *4*, 13556.
[41] K. Klösel, S. Pané, I. A. Mihailovic, C. Hierold, *Electrochim. Acta* **2022**, *403*, 139557.
[42] K. S. Napolskii, I. V. Roslyakov, A. A. Eliseev, D. I. Petukhov, A. V. Lukashin, S.-F. Chen, C.-P. Liu, G. A. Tsirlina, *Electrochim. Acta* **2011**, *56*, 2378.
[43] D. A. Bograchev, T. B. Kabanova, A. D. Davydov, *J. Solid State Electrochem.* **2024**.
[44] L. Wenxin, Z. Wangchen, Z. Yanpeng, L. Yanning, L. Ya, J. Ruomei, Z. Linbo, Z. Li, Z. Peiheng, D. Longjiang, *Nanotechnology* **2019**, *30*, 245702.
[45] R. D. Reeves, L. A. Crosser, G. E. Chester, J. J. Hill, *Nanotechnology* **2017**, *28*, 505401.
[46] A. Fang, M. Haataja, *J. Electrochem. Soc.* **2017**, *164*, D875.
[47] T. T. K. Ingber, M. M. Bela, F. Püttmann, J. F. Dohmann, P. Bieker, M. Börner, M. Winter, M. C. Stan, *J. Mater. Chem. A* **2023**, *11*, 17828.
[48] P. N. Bartlett, R. Beanland, J. Burt, M. M. Hasan, A. L. Hector, R. J. Kashtiban, W. Levason, A. W. Lodge, S. Marks, J. Naik, A. Rind, G. Reid, P. W. Richardson, J. Sloan, D. C. Smith, *Nano Lett.* **2018**, *18*, 941.
[49] P. N. Bartlett, D. A. Cook, Mahboba M. Hasan, A. L. Hector, S. Marks, J. Naik, G. Reid, J. Sloan, D. C. Smith, J. Spencer, Z. Webber, *RSC Adv.* **2017**, *7*, 40720.
[50] C. Li, M. Iqbal, J. Lin, X. Luo, B. Jiang, V. Malgras, K. C. W. Wu, J. Kim, Y. Yamauchi, *Acc. Chem. Res.* **2018**, *51*, 1764.
[51] M. R. Burton, S. J. Richardson, P. A. Staniec, N. J. Terrill, J. M. Elliott, A. M. Squires, N. M. White, I. S. Nandhakumar, *Electrochem. Commun.* **2017**, *76*, 71.
[52] S. Bae, H. Kim, H. S. Lee, *Mater. Chem. Phys.* **2017**, *187*, 82.
[53] R. Hayes, N. Borisenko, M. K. Tam, P. C. Howlett, F. Endres, R. Atkin, *J. Phys. Chem. C* **2011**, *115*, 6855.
[54] L. P. M. dos Santos, R. M. Freire, S. Michea, J. C. Denardin, D. B. Araújo, E. B. Barros, A. N. Correia, P. de Lima-Neto, *J. Mol. Liquids* **2019**, *288*, 111038.
[55] S. C. Perry, J. White, I. Nandhakumar, *Electrochim. Acta* **2023**, *439*, 141674.

[56] R. Al-Salman, H. Sommer, T. Brezesinski, J. Janek, *Chem. Mater.* **2015**, *27*, 3830.
[57] R.-W. Tsai, Y.-T. Hsieh, P.-Y. Chen, I. W. Sun, *Electrochim Acta* **2014**, *137*, 49.
[58] A.-S. Catrangiu, I. Sin, P. Prioteasa, A. Cotarta, A. Cojocaru, L. Anicai, T. Visan, *Thin Solid Films* **2016**, *611*, 88.
[59] F. Golgovici, A. Cojocaru, L. Anicai, T. Visan, *Mater. Chem. Phys.* **2011**, *126*, 700.
[60] L. Thiebaud, S. Legeai, J. Ghanbaja, N. Stein, *Electrochem. Commun.* **2018**, *86*, 30.
[61] L. Piraux, N. Marchal, P. Van Velthem, T. da Câmara Santa Clara Gomes, F. A. Araujo, E. Ferain, J.-P. Issi, V.-A. Antohe, *Nanoscale Adv.* **2025**, *7*, 124.
[62] L. Yang, D. Huh, R. Ning, V. Rapp, Y. Zeng, Y. Liu, S. Ju, Y. Tao, Y. Jiang, J. Beak, J. Leem, S. Kaur, H. Lee, X. Zheng, R. S. Prasher, *Nat. Commun.* **2021**, *12*, 3926.
[63] S. Lal, D. Gautam, K. M. Razeeb, *APL Mater.* **2019**, *7*, 031102.
[64] M. Song, J. Jia, P. Li, J. Peng, X. Pang, M. Qi, Y. Xu, L. Chen, L. Chi, G. Lu, *J. Am. Chem. Soc.* **2023**, *145*, 25570.
[65] R. Ameloot, L. Stappers, J. Fransaer, L. Alaerts, B. F. Sels, D. E. De Vos, *Chem. Mater.* **2009**, *21*, 2580.
[66] M. de Lourdes Gonzalez-Juarez, C. Morales, J. I. Flege, E. Flores, M. Martin-Gonzalez, I. Nandhakumar, D. Bradshaw, *ACS Appl. Mater. Interfaces* **2022**, *14*, 12404.
[67] X. Zhang, J. Maddock, T. M. Nenoff, M. A. Denecke, S. Yang, M. Schroder, *Chem. Soc. Rev.* **2022**, *51*, 3243.
[68] H. Babaei, M. E. DeCoster, M. Jeong, Z. M. Hassan, T. Islamoglu, H. Baumgart, A. J. H. McGaughey, E. Redel, O. K. Farha, P. E. Hopkins, J. A. Malen, C. E. Wilmer, *Nat. Commun.* **2020**, *11*.
[69] M. Hmadeh, Z. Lu, Z. Liu, F. Gándara, H. Furukawa, S. Wan, V. Augustyn, R. Chang, L. Liao, F. Zhou, E. Perre, V. Ozolins, K. Suenaga, X. Duan, B. Dunn, Y. Yamamto, O. Terasaki, O. M. Yaghi, *Chem. Mater.* **2012**, *24*, 3511.
[70] C. Gayner, Y. Amouyal, *Adv. Func. Mater.* **2019**, *30*.
[71] J. F. Serrano-Claumarchirant, M. A. Nasiri, C. Cho, A. Cantarero, M. Culebras, C. M. Gómez, *Adv. Mater. Interface* **2023**, *10*, 2202105.
[72] S. Tajik, H. Beitollahi, F. G. Nejad, I. S. Shoaie, M. A. Khalilzadeh, M. S. Asl, Q. Van Le, K. Zhang, H. W. Jang, M. Shokouhimehr, *RSC Adv.* **2020**, *10*, 37834.
[73] X. Wu, Q. Luo, S. Yin, W. Lu, H. He, C.-Y. Guo, *J. Mater. Sci.* **2021**, *56*, 19311.
[74] J. Hynynen, D. Kiefer, C. Müller, *RSC Adv.* **2018**, *8*, 1593.
[75] C.-Y. Yang, Y.-F. Ding, D. Huang, J. Wang, Z.-F. Yao, C.-X. Huang, Y. Lu, H.-I. Un, F.-D. Zhuang, J.-H. Dou, C.-a. Di, D. Zhu, J.-Y. Wang, T. Lei, J. Pei, *Nat. Commun.* **2020**, *11*, 3292.
[76] V. Vijayakumar, Y. Zhong, V. Untilova, M. Bahri, L. Herrmann, L. Biniek, N. Leclerc, M. Brinkmann, *Adv. Energy Mater.* **2019**, *9*, 1900266.
[77] J. L. Jenkins, P. A. Lee, K. W. Nebesny, E. L. Ratcliff, *J. Mater. Chem. A* **2014**, *2*, 19221.
[78] V. Untilova, J. Hynynen, A. I. Hofmann, D. Scheunemann, Y. Zhang, S. Barlow, M. Kemerink, S. R. Marder, L. Biniek, C. Müller, M. Brinkmann, *Macromolecules* **2020**, *53*, 6314.
[79] V. Untilova, T. Biskup, L. Biniek, V. Vijayakumar, M. Brinkmann, *Macromolecules* **2020**, *53*, 2441.
[80] O. Caballero-Calero, P. Cervino-Solana, P. Cloetens, F. Monaco, M. Martin-Gonzalez, *Appl. Mater. Today.* **2024**, *41*, 102458.
[81] A. Datta, A. Sangle, N. Hardingham, C. Cooper, M. Kraan, D. Ritchie, V. Narayan, S. Kar-Narayan, *Materials* **2017**, *10*, 553.
[82] Z.-P. Chen, Y. Li, C.-Y. Gao, X.-H. Fan, H.-P. Li, L.-M. Yang, *J. Colloid Interface Sci.* **2023**, *646*, 824.
[83] L. Li, N. Shi, X. Jiang, W. Chen, C. Ban, J. Hao, *ACS Appl Mater Interface* **2023**, *15*, 31812.
[84] D. Ni, H. Song, Y. Chen, K. Cai, *J. Materiomics* **2020**, *6*, 364.
[85] A. Sahu, B. Russ, N. C. Su, J. D. Forster, P. Zhou, E. S. Cho, P. Ercius, N. E. Coates, R. A. Segalman, J. J. Urban, *J. Mater. Chem. A* **2017**, *5*, 3346.
[86] J. F. Serrano-Claumarchirant, A. M. Igual-Muñoz, M. Culebras, M. N. Collins, A. Cantarero, C. M. Gómez, *Adv. Mater. Interface* **2021**, *8*, 2100951.
[87] M. Liu, M. Li, R. Wu, P. Liu, C. Liu, *Int. J. Electrochem. Sci.* **2022**, *17*, 221291.
[88] R. Eguchi, K. Hoshino, M. Takashiri, *Sci. Rep.* **2023**, *13*, 5783.
[89] L. Su, Y. X. Gan, *Composites B Eng.* **2012**, *43*, 170.
[90] Y. Sun, Y. Liu, R. Li, Y. Li, S. Bai, *Front. Chem.* **2022**, *10*, 865281.
[91] Y. Bao, Y. Sun, F. Jiao, W. Hu, *Adv. Electron. Mater.* **2023**, *9*, 2201310.
[92] Y. Zhang, S. J. Park, *Polymers* **2019**, *11*, 909.
[93] A. Tripathi, Y. Lee, S. Lee, H. Y. Woo, *J. Mat. Chem. C* **2022**, *10*, 6114.
[94] T.-f. Shi, J.-y. Zheng, X. Wang, P. Zhang, P.-a. Zong, K. M. Razeeb, *Int. Mater. Rev.* **2023**, *68*, 521.
[95] H. Han, L. Zhao, X. Wu, B. Zuo, S. Bian, T. Li, X. Liu, Y. Jiang, C. Chen, J. Bi, J. Xu, L. Yu, *J. Mater. Chem. A* **2024**, *12*, 24041.
[96] R. Singh, S. Dogra, S. Dixit, N. I. Vatin, R. Bhardwaj, A. K. Sundramoorthy, H. C. S. Perera, S. P. Patole, R. K. Mishra, S. Arya, *Hybrid Adv.* **2024**, *5*, 100176.
[97] U. S. Vaitesswar, D. Bash, T. Huang, J. Recatala-Gomez, T. Deng, S.-W. Yang, X. Wang, K. Hippalgaonkar, *Digit Discov.* **2024**, *3*, 210.
[98] G. Han, Y. Sun, Y. Feng, G. Lin, N. Lu, *Adv. Electron. Mater.* **2023**, *9*, 2300042.
[99] A. Baroutaji, A. Arjunan, J. Robinson, M. Ramadan, M. A. Abdelkareem, A. Vance, A. Arafat, A.-G. Olabi, *Sustain. Mat. Technol.* **2024**, *41*, e01008.
[100] A. Danine, J. Schoenleber, J. Ghanbaja, F. Montaigne, C. Boulanger, N. Stein, *Electrochim. Acta* **2018**, *279*, 258.
[101] J. Lee, Y. Kim, L. Cagnon, U. Gösele, J. Lee, K. Nielsch, *Phys. Status Solidi–RRL* **2010**, *4*, 43.
[102] C. V. Manzano, C. L. del Olmo, O. Caballero-Calero, M. Martín-González, *Sustain Energy Fuel* **2021**, *5*, 4597.
[103] L. Ferrer-Argemi, Z. Yu, J. Kim, N. V. Myung, J.-H. Lim, J. Lee, *Sci. Rep.* **2019**, *9*, 9242.
[104] K. Yamauchi, R. Mori, M. Yamaguchi, M. Takashiri, *J. Alloy Comp.* **2019**, *792*, 222.
[105] Z. G. Zou, K. F. Cai, S. Chen, Z. Qin, *Mater. Res. Bull.* **2012**, *47*, 3292.
[106] C. Lei, M. R. Burton, I. S. Nandhakumar, *Phys. Chem. Chem. Phys.* **2016**, *18*, 14164.
[107] N. Padmanathan, S. Lal, D. Gautam, K. M. Razeeb, *ACS Appl. Electron. Mater.* **2021**, *3*, 1794.
[108] F. Li, G. Jinghan, W. Wang, Y. Gong, *Int. J. Electrochem. Sci.* **2022**, *17*, 221055.
[109] S. Lal, K. M. Razeeb, D. Gautam, *ACS Appl. Energy Mater.* **2020**, *3*, 3262.
[110] T. Wu, H.-K. Lee, N. V. Myung, *J. Electrochem. Soc.* **2016**, *163*, D801.
[111] K.-J. Shin, T.-S. Oh, *J. Electron Mater.* **2015**, *44*, 2026.
[112] B. Abad, M. Rull-Bravo, S. L. Hodson, X. Xu, M. Martin-Gonzalez, *Electrochim. Acta* **2015**, *169*, 37.
[113] M. Culebras, C. M. Gómez, A. Cantarero, *J. Mater. Chem. A* **2014**, *2*, 10109.
[114] W. Yang, H. Xu, Y. Li, W. Wang, *J. Electron Mater.* **2017**, *46*, 4815.
[115] Y. Li, C.-Y. Gao, X.-H. Fan, L.-M. Yang, *Synth. Mater.* **2021**, *282*, 116949.
[116] J. Zhang, G. Song, L. Qiu, Y. Feng, J. Chen, J. Yan, L. Liu, X. Huang, Y. Cui, Y. Sun, W. Xu, D. Zhu, *Macromol. Rapid Commun.* **2018**, *39*, 1800283.
[117] Z.-P. Chen, C.-Y. Gao, Y. Li, H.-P. Li, X.-H. Fan, L.-M. Yang, *J. Alloys Compd.* **2024**, *988*, 174297.
[118] L. Li, S. Xu, G. Li, *Energy Technol.* **2015**, *3*, 825.
[119] T. Chang, S. Cho, J. Kim, J. Schoenleber, C. Frantz, N. Stein, C. Boulanger, W. Lee, *Electrochim. Acta* **2015**, *161*, 403.
[120] P. Kumar, M. Pfeffer, N. Peranio, O. Eibl, S. Bäßler, H. Reith, K. Nielsch, *Acta Mater.* **2017**, *125*, 238.
[121] Y. Yang, D. K. Taggart, M. A. Brown, C. Xiang, S.-C. Kung, F. Yang, J. C. Hemminger, R. M. Penner, *ACS Nano* **2009**, *3*, 4144.
[122] D. Pinisetty, M. Gupta, A. Karki, D. Young, R. Devireddy, *J. Mater. Chem.* **2011**, *21*, 4098.
[123] Y. Li, C.-Y. Gao, X.-H. Fan, H.-P. Li, L.-M. Yang, *Adv. Mater. Technol.* **2023**, *8*, 2201544.
[124] S. Yin, W. Lu, X. Wu, Q. Luo, E. Wang, C.-Y. Guo, *ACS Appl. Mater. Interface* **2021**, *13*, 3930.
[125] S. Yin, W. Lu, R. Wu, W. Fan, C.-Y. Guo, G. Chen, *ACS Appl. Mater. Interface* **2020**, *12*, 3547.
[126] Y. Li, C.-Y. Gao, X.-H. Fan, L.-M. Yang, *Chem. Eng. J.* **2022**, *443*, 136536.

Manuscript received: February 6, 2025
Revised manuscript received: April 22, 2025
Version of record online: